J Neurosurg 102:664–672, 2005

Combined use of tractography-integrated functional neuronavigation and direct fiber stimulation

Kyousuke Kamada, M.D., Tomoki Todo, M.D., Yoshitaka Masutani, Ph.D., Shigeki Aoki, M.D., Kenji Ino, R.T., Tetsuya Takano, Ph.D., Takaaki Kirino, M.D., Nobutaka Kawahara, M.D., and Akio Morita, M.D.

Departments of Neurosurgery and Radiology, The University of Tokyo; and Kobayashi Sofamor-Danek, Tokyo, Japan

Object. The aim of this study was better preoperative planning and direct application to intraoperative procedures through accurate coregistration of diffusion-tensor (DT) imaging–based tractography results and anatomical three-dimensional magnetic resonance images and subsequent importation of the combined images to a neuronavigation system (functional neuronavigation).

Methods. Six patients with brain lesions adjacent to the corticospinal tract (CST) were studied. During surgery, direct fiber stimulation was used to evoke motor responses to confirm the accuracy of CST depicted on functional neuronavigation. In three patients, stimulation of the supposed CST elicited the expected motor evoked potentials. In the other three, stimulation at the resection borders more than 1 cm away from the supposed CST showed no motor response. All patients underwent appropriate tumor resection with preservation of the CST.

Conclusions. Integration of the DT imaging–based tractography information into a traditional neuronavigation system demonstrated spatial relationships between lesions and the CST, allowing for the avoidance of tract injury during lesion resection. Direct fiber stimulation was used for real-time reliable white matter mapping, which served to adjust for any discrepancy between the neuronavigation system data and potentially shifted positions of the brain structures. The combination of these techniques enabled the authors to identify accurate positions of the CST during surgery and to accomplish optimal tumor resections.

Key Words • corticospinal tract • diffusion-tensor imaging • fiber stimulation • functional neuronavigation • tractography

Preserving brain functions while maximizing the extent of tumor resection is the basic strategy in prolonging survival as well as maintaining quality of life in patients.[7] To preserve eloquent brain functions, it is important to identify not only the eloquent cortices, but also the subcortical fiber connections. Visualization of the spatial relationships between the eloquent structures and a lesion allows for optimal resection.

Anisotropic diffusion-weighted imaging is dependent on the directions of water molecule diffusion in the white matter (anisotropic diffusion), which is attributed to the organization of axonal fibers and their myelin sheaths. Craniocaudally oriented fiber tracts present high raw signal intensity when diffusion-sensitizing gradients are oriented perpendicular to the tracts. Authors of previous reports have indicated that the craniocaudally oriented fiber tracts might be used to reveal the CST on the basis of lesion analyses.[10] Furthermore, several groups extracted the hyperintense areas, assuming that they might be the CST, and fused them with anatomical images on a neuronavigation system.[4,9] Recently developed fiber-tracking processes (tractography) demonstrate the major axonal fascicles of interest by calculating DT and measuring changes in the nuclear MR signal with diffusion sensitization along at least six noncolinear directions.[1] Many groups have used DT imaging–based tractography to visualize the spatial relationship between lesions adjacent to the sensorimotor system and the CST for presurgical planning and functional prediction.[11,15,16,18] Note, however, that it is technically difficult to integrate DT imaging–based tractography data into a neuronavigation system. Furthermore, no physiological data have confirmed the accuracy of the CST as depicted using either DT imaging–based tractography or simple anisotropic diffusion-weighted imaging based on electrophysiological techniques such as direct fiber stimulation.

In the present study, we accurately coregistered DT imaging–based tractography results and anatomical 3D MR images and successfully demonstrated the white matter connections on a neuronavigation system. In addition, the accuracy of the CST depicted was confirmed by recording MEPs activated by direct fiber stimulation. We describe herein the usefulness and reliability of real-time functional neuronavigation through the use of DT imaging–based tractography and fiber stimulation.

Abbreviations used in this paper: CST = corticospinal tract; DT = diffusion tensor; DTPA = diethylenetriamine pentaacetic acid; FA = fractional anisotropy; FOV = field of view; GBM = glioblastoma multiforme; MEP = motor evoked potential; MR = magnetic resonance; SSEP = somatosensory evoked potential; 3D = three-dimensional.

Clinical Material and Methods

Patient Population

We examined six patients with space-occupying lesions in the brain affecting the primary motor area and the CST. Demographic data in all patients are summarized in Table 1. The lesion types consisted of ganglioglioma (one lesion), cavernous angioma (one lesion), GBM (three lesions), and metastatic brain tumor (one lesion). The study was approved by the institutional review board, and written informed consent was obtained from each patient and/or a family member before participation.

Magnetic Resonance Imaging Protocols

All MR imaging studies were performed as a single experiment on a 1.5-tesla whole-body MR unit with echo planar capabilities and a standard whole-head transmitter/receiver coil (Signa Echospeed; General Electric Medical Systems, Milwaukee, WI).

Diffusion-Tensor Imaging

We obtained single-shot spin echo–echo planar sequences (TR 5000 msec, TE 96 msec, acquisitions 26 interleaved contiguous 4-mm axial images) with no cardiac triggering. A data matrix of 128 × 128 over an FOV of 240 × 240 mm was obtained, acquiring 128 echoes per excitation. Diffusion gradients were applied in 12 noncolinear independent axes by using a b value of 0 and 1000 seconds/ mm^2. A single echo planar imaging set took 25 seconds and was repeated six times to increase the signal-to-noise ratio. Realignment of these 13 DT imaging sets and compensation for eddy current–induced morphing were performed on the basis of the T_2-weighted echo planar imaging set (b value = 0) on a workstation equipped with the MR unit. Compensation was performed by maximizing the mutual information between T_2-weighted echo planar and other echo planar imaging data sets with diffusion gradients. We obtained anatomical 3D MR images of each patient's head, consisting of 128 sequential, 1.5-mm-thick axial slices with a resolution of 256 × 256 pixels over an FOV of 240 mm with 3D spoiled gradient–recalled acquisition in the steady-state sequence. During the entire MR imaging session, foam cushions were used to immobilize the patient's head.

Diffusion Tensor Calculation and DT Imaging–Based Fiber Tracking

The DT imaging data sets and 3D MR images were analyzed using freeware for diffusion tensor analysis and fiber tracking (Volume One and dTV; URL: http://volume-one.org).[11,14] In the software, six elements of the symmetric 3 × 3 matrix of DT at each voxel were determined according to the least-square fit, and the DT was diagonalized to obtain three eigenvalues and three eigenvectors.[1,14] An eigenvector ($e1$) associated with the largest eigenvalue ($\lambda 1$) was assumed to represent the local fiber direction. Anisotropy maps were obtained using orientation-independent FA.

Fiber tracking was initiated from a manually selected seed area from which lines were propagated in both anterograde and retrograde directions according to $e1$ at each pixel (Fig. 1). To depict the motor tracts, the seed area was placed on the cerebral peduncle where the CST is known to run, while observing the color encoded fiber orientation map.

TABLE 1

Demographic data in six patients who underwent functional neuronavigation

Case No.	Age (yrs), Sex	Lesion Location	Symptom	Histological Diagnosis
1	23, M	rt thalamus	lt numbness	ganglioglioma
2	74, M	rt parietal region	lt hemiparesis (subcortical hematoma)	cavernous angioma
3	48, M	rt temporoparietal region	confusion & lt hemiparesis	GBM
4	62, F	lt parietal region	mild confusion & rt hemiparesis	GBM
5	57, M	lt frontotemporal region	mild confusion	GBM
6	52, M	rt parietal region	lt hemiparesis	metastatic tumor

Cortical target regions were carefully placed in the suspected primary motor area. We used the two-regions-of-interest method (that is, seed and target regions) to demonstrate only the descending fibers from the primary motor area to the cerebral peduncle.[5,11,14] Tracking was terminated when it reached a pixel with an FA lower than 0.18. Tract reconstruction required approximately 30 seconds by using a personal computer with a 3-GHz Pentium 4 processor and 2 GB RAM.

Voxelization, Image Registration, and Data Fusion

After fiber tracking of the CST, voxels containing tract fibers were marked in a volume data whose matrix size was the same as that for DT imaging; that is, voxelization of tracking lines was performed. The voxels were also colored based on the degree of anisotropy in each voxel (Fig. 1B). Red represents high anisotropy, whereas yellow and white represent middle and low anisotropy, respectively. For the coregistration of the voxelized tracts and 3D MR imaging data, coregistration between T_2-weighted echo planar imaging data and 3D MR imaging data was performed first, based on the maximization of mutual information and by affine transformation of the former data.[3,13] Because voxelized CST data were in the same coordinate system as the T_2-weighted echo planar imaging data, the volume data of the voxelized tracts as well as the T_2-weighted echo planar imaging data were transformed. After the registration process, the results were visually evaluated by at least two radiologists and one neurosurgeon. Finally, the voxelized CST data and the anatomical 3D MR imaging data were simply fused and resliced (128 slices) with DICOM format, according to the original 3D MR imaging header information (Fig. 2).

Functional Neuronavigation

The resliced 3D MR imaging data together with the functional information were transferred via fast ethernet to a neuronavigation system (StealthStation; Medtronic Sofamor-Danek, Memphis, TN). A program on the navigation system segmented the tract information by setting the signal thresholds and colored the CST green.

The entire functional neuronavigation procedure can be summarized as follows: 1) fiber tracking; 2) voxelization of CST; 3) image registration (3D MR imaging data and DT

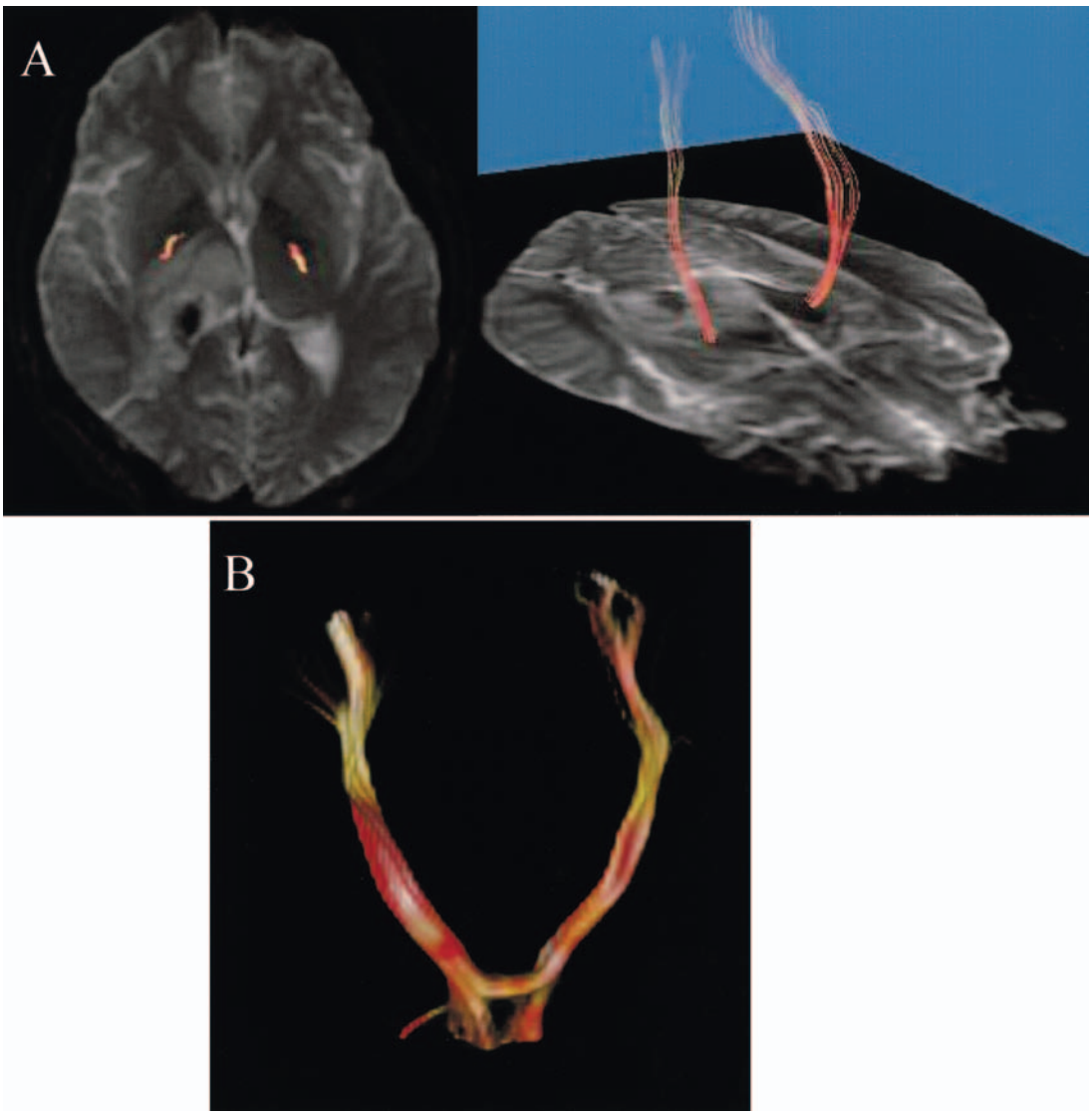

FIG. 1. Case 1. A: Diffusion-tensor imaging–based tractography data indicating that the CST has shifted anteriorly. B: Three-dimensionally reconstructed CST voxels clearly demonstrating the CST profiles in both hemispheres.

imaging data); 4) fusion of CST and 3D MR imaging data; 5) reslicing the fused MR imaging data; and 6) importing the resliced MR imaging data to the neuronavigation system.

Cortical and Subcortical Mapping

Patients underwent surgery while in a state of general anesthesia with the continuous infusion of propofol. No muscle relaxant was used except during the introduction of anesthesia. After craniotomy, cortical mapping was performed through SSEPs and MEPs (Neuropack; NihonKoden, Tokyo, Japan). Phase reversals of the cortical SSEPs were observed to identify the central sulcus with a strip electrode consisting of four channels placed on the brain surface. During stimulation, we applied 200 repetitions of a 0.2-msec constant-current pulse (frequency 5.1 Hz, current 15 mA) delivered to the median nerve at the wrist. The electrode was placed at several different locations, including the suspected primary somatosensory, motor, and surrounding areas before resection. We identified the location at which the SSEP electrode generated the highest N20-amplitudes (active SSEP electrode). One of the electrode channels just anterior to the active SSEP electrode was placed on the suspected motor cortex for cortical stimulation. Monopolar stimulation with five trains of monophasic square-wave pulses was applied with a frequency of 1 Hz. The duration of each pulse was 0.2 msec and the current amplitudes varied from 3 to 25 mA. Electromyograms of the MEPs were monitored using needle electrodes subdermally placed in the palm and the sole of patients. During tumor resection, cortical SSEPs and MEPs were continuously monitored on cortical stimulation.

When the resection approached the CST on neuronavigation, direct fiber stimulation was performed to identify tract connections. For direct fiber stimulation, monopolar stimulation in five trains of monophasic square-wave pulses was applied with a frequency of 1 Hz. The duration of each

pulse was 0.2 msec and the current amplitudes varied from 1 to 25 mA. The electric fiber stimuli were applied at several locations in the resection cavity through another strip electrode (cathode) to evoke MEPs at the palm and sole. The reference needle electrode (anode) was subdermally placed at the margin of the skin incision. Ten responses by fiber stimulation were averaged to obtain stable MEP results.

Illustrative Cases

Case 1

This 23-year-old man who had experienced diplopia and numbness in his left extremities for more than 3 months underwent an open biopsy of a right thalamic tumor at another hospital. The biopsy failed to provide a histopathological diagnosis, and so he was referred to our hospital for diagnosis and treatment of the tumor. The T_1-weighted MR imaging studies revealed a well-demarcated hypointense tumor mainly in the right thalamus with mild, ring-like Gd-DTPA enhancement. The tumor demonstrated homogeneous hyperintensity with little peritumoral edema on T_2-weighted MR images (Figs. 1 and 2). Diffusion-tensor imaging–based tractography data demonstrated that the CST was adjacent to the tumor and slightly shifted anteriorly (Figs. 2 and 3). The tumor was approached via a right parietal corticotomy.

While approaching the tumor by a route more than 2 cm away from the CST as displayed on the neuronavigation system, we observed no change in the amplitude or latency of SSEPs and MEPs with the application of cortical stimulation. While dissecting the anterior border of the well-demarcated tumor, the amplitudes of the MEPs on cortical stimulation (15 mA) decreased to half the preresection level, although there was no change in the SSEPs. After gross removal of the tumor, direct fiber stimulation was applied at several points inside the cavity to verify the CST location and profile. We observed obvious MEP responses in the palm and sole with fiber stimulation at the anterior wall of the tumor cavity, the site matching the CST position indicated on DT imaging–based tractography. The minimal threshold of the fiber stimulation was 12 mA. No response was noted at the posterior and medial walls at 25 mA in stimulus intensity (Fig. 4). The distance between the anterior stimulus point and the posterior CST border was within 5 mm on the neuronavigation image.

Postoperatively, the patient experienced moderate left hemiparesis that improved over 2 months. The histopathological diagnosis was ganglioglioma. Diffusion-tensor imaging–based tractography after surgery revealed preservation of the CST, although its density was slightly reduced when the same seed area, target area, and FA as those on the preoperative evaluation were used for CST detection (Fig. 5).

Case 4

This 62-year-old right-handed woman suffered from disorientation and mild right hemiparesis for more than 2 months prior to clinical examination. A routine MR imaging study revealed ring-like enhancement on T_1-weighted images with contrast medium, and what was supposed to be a high-grade glioma appeared to be located adjacent to the CST in the deep white matter.

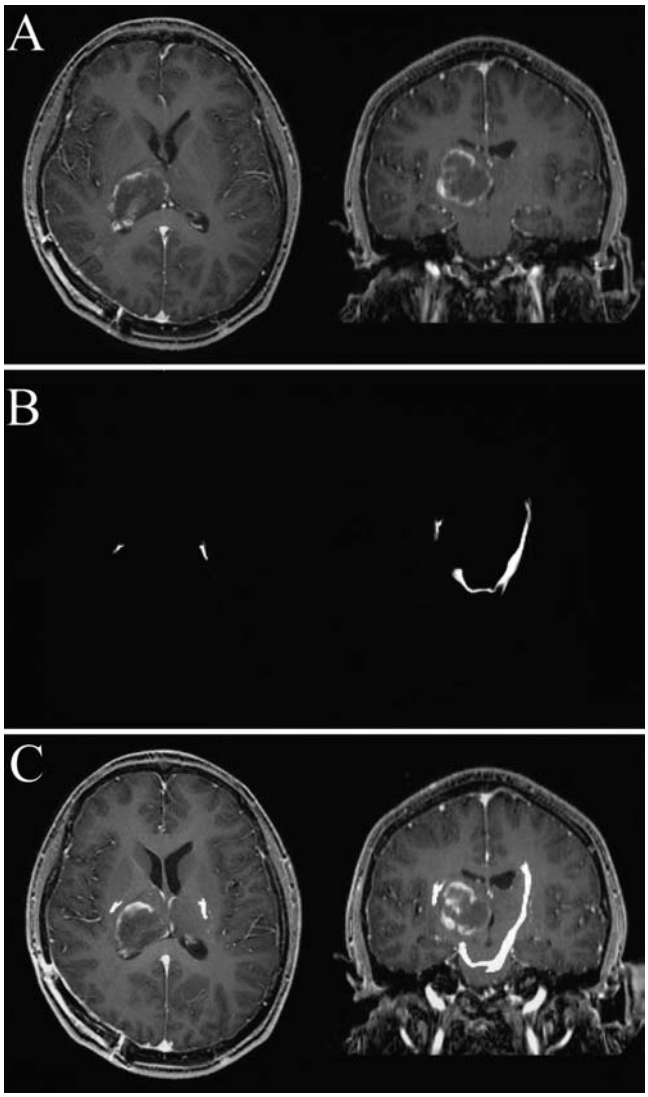

FIG. 2. Case 1. A: Transverse *(left)* and coronal *(right)* T_1-weighted 3D MR images with Gd-DTPA enhancement. B: Marked voxels of the CST on DT imaging–based tractography in the same orientations as those featured in A. C: Results of 3D MR imaging fused with those of DT imaging–based tractography, revealing the anterior shift of the CST.

Three-dimensionally reconstructed MR images on the neuronavigation system delineated the spatial relationship of the CST (green) and the tumor (yellow; Fig. 6). During surgery while extirpating the tumor, we observed no change in the amplitude and latency of the cortical SSEPs and MEPs. After gross-total removal of the tumor, the anterior border of resection was approximately 1.5 cm away from the CST on neuronavigation images. Direct fiber stimulation at the maximal stimulus amplitude (25 mA) did not evoke MEPs in the palm or sole. The patient showed no neurological deterioration after surgery.

Case 6

This 52-year-old right-handed man underwent stereotactic radiosurgery 1 year previously for lung cancer metastatic to the right parietal region. Despite treatment the tumor

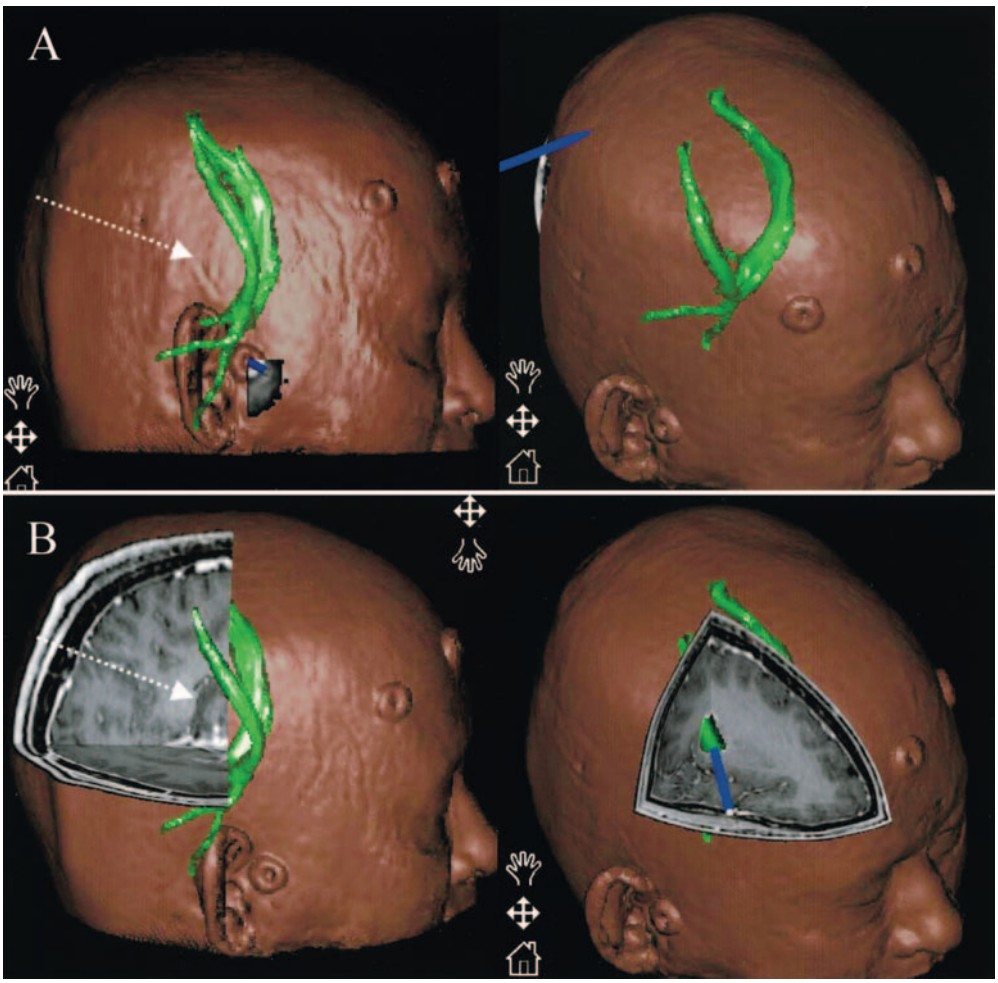

FIG. 3. Case 1. Three-dimensionally reconstructed whole-head MR imaging data on the neuronavigation system, both the plain mode (A) and the cut mode (B), displaying the CST (green). *White arrows* indicate the surgical route for approaching the thalamic tumor.

size increased and a left hemiparesis gradually worsened. A routine MR imaging study demonstrated ring-like enhancement of the lesion with contrast enhancement as well as marked surrounding edema. Diffusion-tensor imaging–based tractography revealed that the tumor was located adjacent to the CST in the deep white matter (Fig. 7A).

During surgery while extirpating the tumor, we observed no change in the amplitude and latency of the cortical SSEPs and MEPs. After total removal of the tumor, the anterior border of the resection margin was approximately 0.5 cm away from the CST on the neuronavigation image (Fig. 7B). Direct fiber stimulation evoked MEPs in the left hand and sole at an amplitude as low as 3 mA, which indicated that the CST was very close but that the connections were spared. The patient temporarily experienced severe hemiparesis postoperatively, but he recovered and was able to walk with little support within 1 month.

Results

Corticospinal Tractography

For all patients, we fused DT imaging–based tractography data with anatomical 3D MR imaging information after distortion correction and image registration. The entire procedure, including image registration, fiber tracking, exportation of tract data, and 3D reconstruction on the neuronavigation system, was accomplished within 1 hour after acquisition of the MR imaging data. In Case 1, in which the distance between the resection margin and the CST was less than 0.5 cm on neuronavigation images, the MEP amplitudes decreased as much as 50% during intraoperative monitoring. Although fiber stimulation of the CST had evoked MEPs in the patient's left palm and sole, he suffered from mild transient hemiparesis after tumor resection. Cases 5 and 6 delineated the obvious MEPs by fiber stimulation in which the distance between the resection margin and the CST was 1.0 and 0.5 cm, respectively, on neuronavigation images. These two cases demonstrated maximal tumor resection with favorable functional prognosis.

In Cases 2, 3, and 4, the amplitudes and latencies of cortical SSEPs and MEPs on cortical stimulation were preserved throughout surgery. Fiber stimulation elicited no MEPs, and the distances between the resection margins and the CST were approximately 1.0, 1.5, and 1.5 cm, respectively, on neuronavigation images. None of the patients in

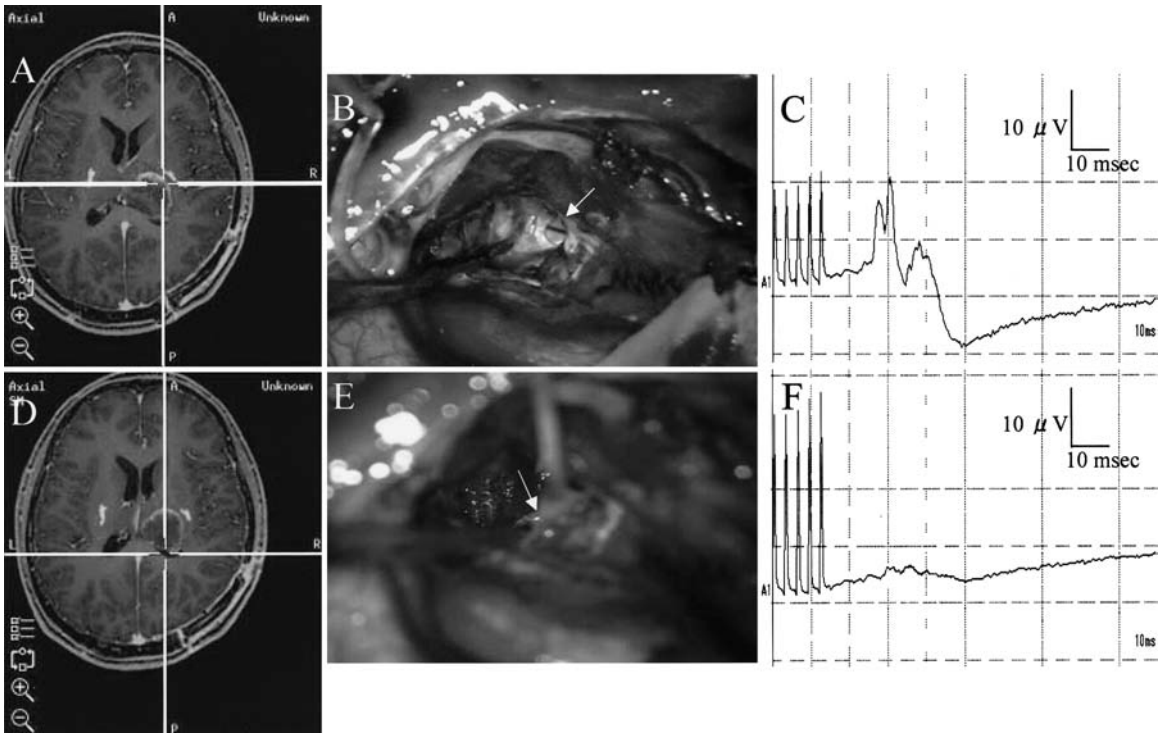

FIG. 4. Case 1. A: A T_1-weighted MR image demonstrating the electrode position for fiber stimulation at the anterior wall of the resection cavity *(white cross)*. B: Intraoperative photograph illustrating placement of an electrode *(arrow)* at the anterior wall of the tumor cavity. C: Electromyogram demonstrating the MEPs elicited by direct fiber stimulation at the anterior wall of the tumor cavity. D: A T_1-weighted MR image exhibiting the electrode position at the posterior wall of the cavity *(white cross)*. E: Intraoperative photograph displaying placement of an electrode *(arrow)* at the posterior wall of the tumor cavity. F: Electromyogram revealing no MEP on stimulation of the posterior cavity wall.

these cases exhibited neurological deficits after surgery. These findings indicate that the CST depicted on DT imaging–based tractography accurately reflects the actual position of the CST in the brain. Surgical procedures performed within approximately 0.5 cm of the CST, as depicted on tractography-integrated neuronavigation images, might cause at least transient functional damage to the CST.

Results of fiber stimulation and each patient's prognosis are summarized in Table 2.

Discussion

In this study, we established a useful neurosurgical technique of DT imaging–based tractography data integrated in-

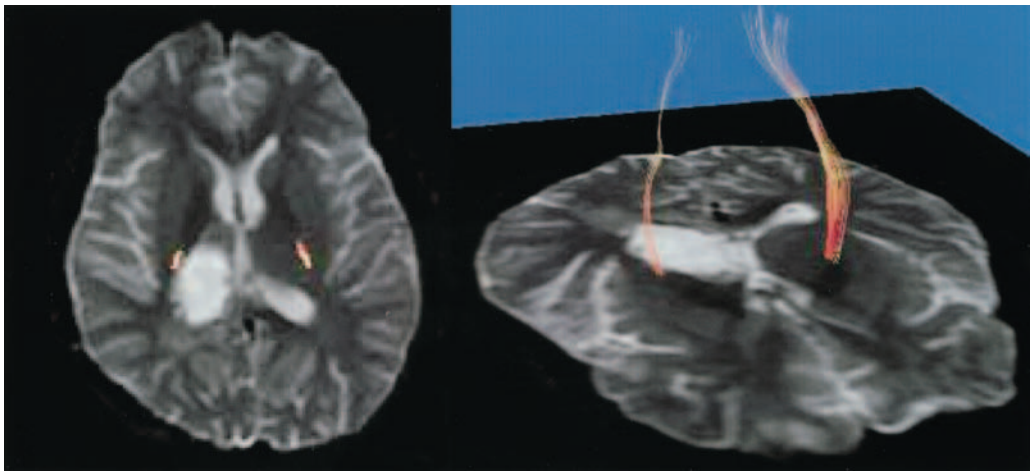

FIG. 5. Case 1. Postoperative T_2-weighted MR images with the superimposed CST demonstrating that the preserved CST remains anterior to the tumor cavity.

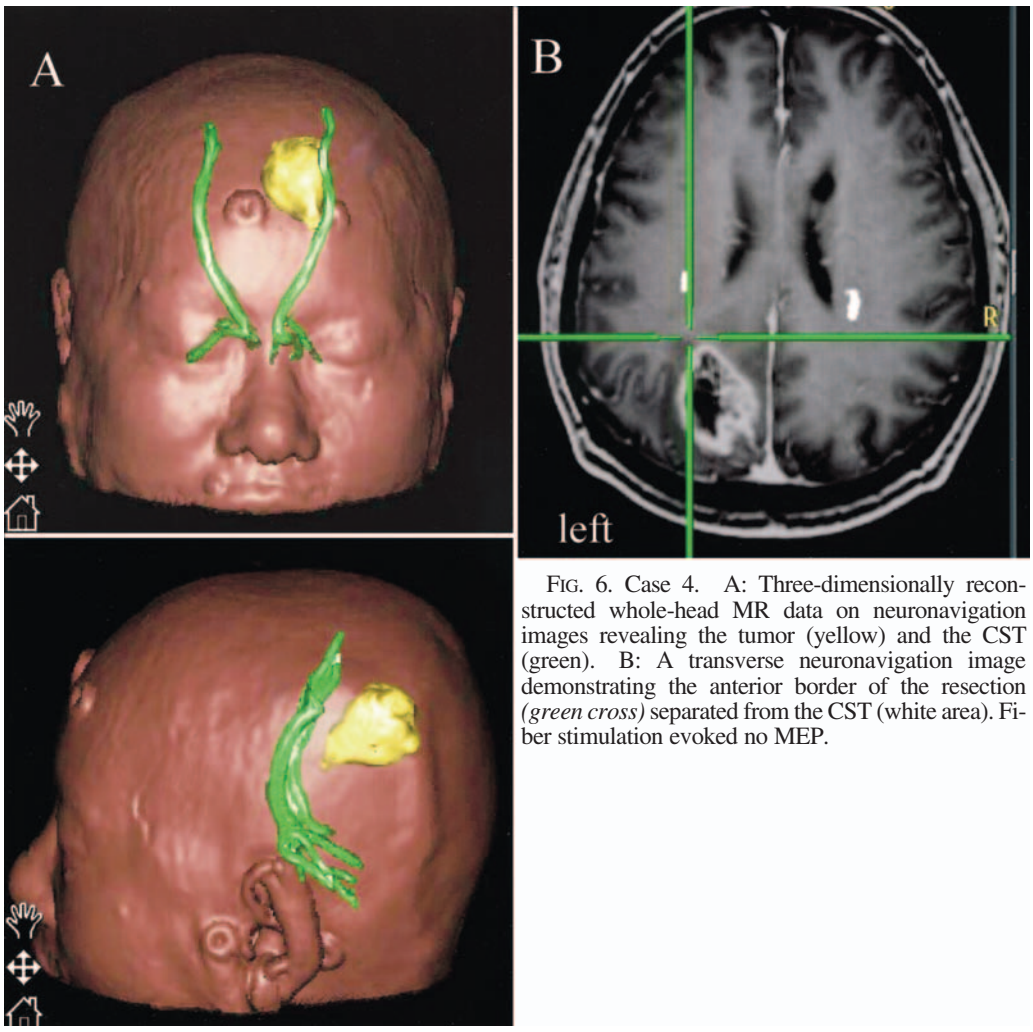

FIG. 6. Case 4. A: Three-dimensionally reconstructed whole-head MR data on neuronavigation images revealing the tumor (yellow) and the CST (green). B: A transverse neuronavigation image demonstrating the anterior border of the resection *(green cross)* separated from the CST (white area). Fiber stimulation evoked no MEP.

to a functional neuronavigation system and intraoperative MEP monitoring by direct fiber stimulation. In the cases presented, the CST depicted on the neuronavigation images reliably reflected the anatomical CST. We believe that this technique is a powerful tool for neurosurgeons in making accurate decisions about resecting deep-seated lesions without risking injury to the CST.

Tumor resection in functional areas involving eloquent subcortical fibers presents a high risk of neurological consequences, despite preservation of eloquent cortices. Several authors have asserted that intraoperative fiber stimulation might be used to perform subcortical functional mapping to avoid injury to the CST.[6] Duffau, et al., indicated that direct fiber stimulation is safe, accurate, and reliable in detecting subcortical pathways related to motor and language functions. We used this method in our technique to allow for accurate decision making based on real-time information on functional pathways. Technical difficulties regarding direct fiber stimulation included searching for optimal stimulus points and continuous MEP monitoring. Targeted tracts such as the CST are visually indistinguishable from other white matter tissue. In addition, searching and stimulating tract fibers require interruption of resection procedures, resulting in a longer operation time. It was therefore desirable to know the anatomical relationship between a tumor and the tract distributions before and during surgery.

Although the CST is the biggest axonal bundle in the human brain, descending tracts in the cerebral peduncle originate from various cortices such as the frontal and parietal lobules.[17] Maier, et al.,[12] made a quantitative comparison of the density of the CST projections from the primary motor area and that of the supplementary motor area to the spinal motor nuclei by densitometric analyses in macaque monkeys, which revealed that the former was much denser than the latter. Others have reported that only approximately 20% of the CST originates from the somatosensory cortex.[4] These data corroborate that the cerebral peduncle at the midbrain is largely dominated by the CST originating from the primary motor area. Appropriate selections of the seed area (cerebral peduncle) and the target area (primary motor area) enable marking of the correct CST.[5] In support of this finding, direct fiber stimulation applied to the walls of the resection cavity in Cases 1, 5, and 6 efficiently elicited MEPs. In all cases in the present study, the combination of direct fiber stimulation and DT imaging–based fiber tracking potentiated real-time functional neuronavigation for deep-seated lesions.

Berman, et al.,[2] recently reported on the use of DT im-

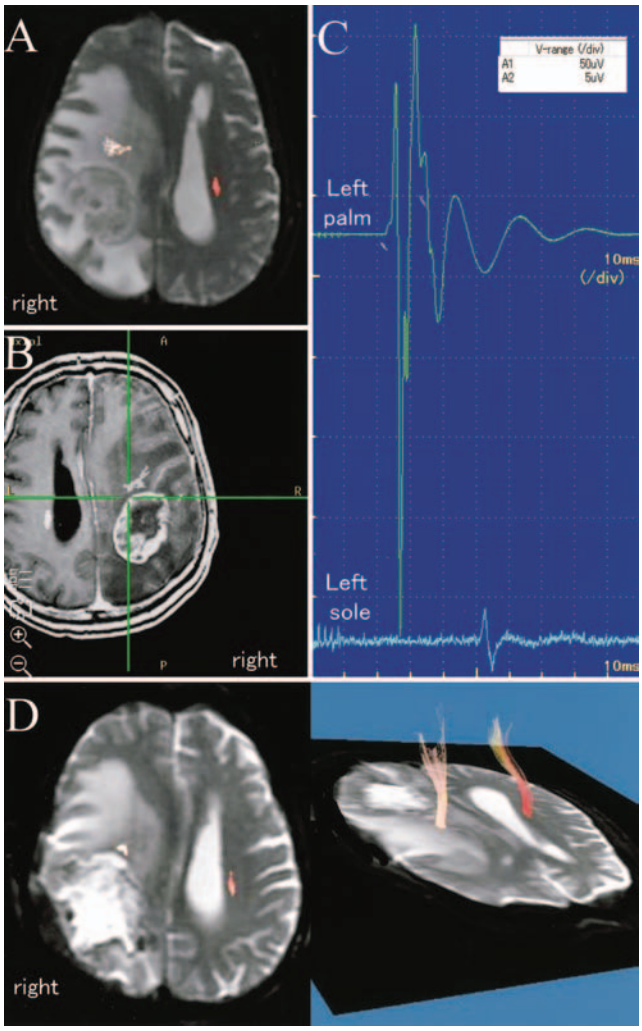

FIG. 7. Case 6. A: Diffusion-tensor imaging–based tractography data indicating that the CST has shifted anteriorly. B: A T_1-weighted MR image from the functional neuronavigation system revealing the electrode position for fiber stimulation at the anterior wall of the resection cavity *(green cross)*. C: Electromyogram demonstrating the MEPs in the palm and sole elicited by direct fiber stimulation at the anterior cavity wall. D: Postoperative T_2-weighted MR image with the superimposed CST demonstrating that the preserved CST remains anterior to the cavity.

aging–based tractography and intraoperative cortical stimulation mapping, demonstrating the usefulness of these techniques in glioma surgery. Data in the present study add electrophysiological validation of the illustrated fiber information through direct fiber stimulation, thus justifying the use of DT imaging–based fiber tracking for various presurgical plannings. Moreover, direct fiber stimulation is an excellent means of identifying anatomical profiles of the CST in relation to the resection cavity and therefore may be more practical during surgery compared with the use of MEPs by cortical stimulation. Awake surgery is another method of directly monitoring motor functions, although this procedure accompanies certain risks related to anesthesia and can be applied in a limited number of patients who can cooperate during the operation. Note, however, that monitoring through awake surgery is known often to show false-positive signs due to varying patient conditions. In comparison, the present technique is less invasive and provides stable responses of the CST.

TABLE 2

Results of fiber stimulation on functional neuronavigation

Case No.	MEP on Fiber Stimulation		Functional Prognosis
	Distance Btwn CST & Resection Margin (cm)	Minimal Threshold (mA)	
1	0.5	12	transient hemiparesis
2	1.0	negative	condition improved
3	1.5	negative	condition improved
4	1.5	negative	condition improved
5	1.0	20	no deterioration
6	0.5	3	condition improved

In practice, a major problem of neuronavigation is shifting of the brain structures during surgery. In fact, we observed cortical areas that shifted to some extent in all cases during resection. The medial side of the tumor exhibited little shifting, which was confirmed by the locations of the ventricles and midbrain on a computerized tomography scan acquired immediately after surgery and on an intraoperative ultrasonogram, corresponding to their locations on the neuronavigation images. Structures close to the midline including the CST are less prone to shifting than those near the surface, because of the firm supporting structures such as the falx, the tentorium cerebelli, and the contralateral cerebral hemisphere. Nevertheless, ways to incorporate feedback information on intraoperative brain structure shifting are in development to refine the proposed neuronavigation system. Note that an accurate reflection of brain shifting in our technique of real-time tractography-guided navigation may be obtained in the near future by incorporating information from an intraoperative MR imager.

Echo planar imaging can minimize motion artifacts and is indispensable for DT imaging data acquisition. A critical issue with this technique is the geometric distortion induced by magnetic field heterogeneity and a motion-probing gradient, although there are several ways to minimize the scanning artifact such as homogenization of the static magnetic field and morphing compensation. Nevertheless, it is important to address this issue of image distortion more carefully by developing a better shielding system and new sequences such as parallel imaging.[8]

The fiber orientation depicted on DT imaging–based tractography reflects the average orientation of axonal fibers in each pixel and is susceptible to the extent of tissue heterogeneity. Within a pixel exists a minor portion of fibers that run in a different direction from the majority of fibers. Therefore, at the present time, tractography can only provide gross anatomical information on major tracts in the white matter. With regard to the CST, DT imaging–based tractography tends to trace the straight route (craniocaudal direction) better than the curved one (right–left direction) and it is difficult to differentiate the CST projections for the hand compared with those for the foot or other body areas. Hence, numerical analyses of the distances between the CST on DT imaging–based tractography and the resection borders should be carefully interpreted. In our DT study, however, the spatial resolution was sufficient to demonstrate the CST. Diffusion-tensor imaging–based tractogra-

phy awaits further improvement in quality through the use of new techniques such as high angular sampling of motion-probing gradients, interpolation, or regularization of tensor fields.

We reported on a novel procedure for importing DT imaging–based tractography data into a neuronavigation system and confirmed the CST location through intraoperative direct fiber stimulation. The functionally oriented neuronavigation technique enabled us quickly to identify the CST in the white matter during surgery. As a result, we accomplished optimal resections of mass lesions, sparing the adjacent CST. Note that the accumulation of additional cases is underway. Moreover, the technique may be applied to other neuronal tracts such as those for visual and language functions, leading to further progress in functional neuronavigation.

Conclusions

Integration of the CST on DT imaging–based tractography into a traditional neuronavigation system was valuable for making neurosurgical strategies, especially in preoperative planning. Direct fiber stimulation confirmed that the illustrated CST reflected the actual CST in the white matter, proving that functional neuronavigation together with DT imaging–based tractography is a reliable tool. Although anatomical relationships between the surgical target and fiber tracts established preoperatively may be compromised by intraoperative brain shifts, the use of direct fiber stimulation at least partially compensated for the problem by locating the CST in relation to the resected cavity.

References

1. Basser PJ, Mattiello J, LeBihan D: MR diffusion tensor spectroscopy and imaging. **Biophys J 66:**259–267, 1994
2. Berman JI, Berger MS, Mukherjee P, Henry RG: Diffusion-tensor imaging-guided tracking of fibers of the pyramidal tract combined with intraoperative cortical stimulation mapping in patients with gliomas. **J Neurosurg 101:**66–72, 2004
3. Chen HM, Varshney PK: Mutual information-based CT-MR brain image registration using generalized partial volume joint histogram estimation. **IEEE Trans Med Imaging 22:**1111–1119, 2003
4. Coenen VA, Krings T, Axer H, Wiedermann J, Kranzlein H, Hans FJ, et al: Intraoperative three-dimensional visualization of the pyramidal tract in a neuronavigation system (PTV) reliably predicts true position of principal motor pathways. **Surg Neurol 60:** 381–390, 2003
5. Conturo TE, Lori NF, Cull TS, Akbudak E, Snyder AZ, Shimony JS, et al: Tracking neuronal fiber pathways in the living human brain. **Proc Natl Acad Sci USA 96:**10422–10427, 1999
6. Duffau H, Capelle L, Sichez N, Denvil D, Lopes M, Sichez JP, et al: Intraoperative mapping of the subcortical language pathways using direct stimulations. An anatomo-functional study. **Brain 125:**199–214, 2002
7. Hentschel SJ, Sawaya R: Optimizing outcomes with maximal surgical resection of malignant gliomas. **Cancer Control 10:** 109–114, 2003
8. Jaermann T, Crelier G, Pruessmann KP, Golay X, Netsch T, van Muiswinkel AM, et al: SENSE-DTI at 3 T. **Magn Reson Med 51:**230–236, 2004
9. Kamada K, Houkin K, Takeuchi F, Ishii N, Ikeda J, Sawamura Y, et al: Visualization of the eloquent motor system by integration of MEG, functional, and anisotropic diffusion-weighted MRI in functional neuronavigation. **Surg Neurol 59:**352–362, 2003
10. Karibe H, Shimizu H, Tominaga T, Koshu K, Yoshimoto T: Diffusion-weighted magnetic resonance imaging in the early evaluation of corticospinal tract injury to predict functional motor outcome in patients with deep intracerebral hemorrhage. **J Neurosurg 92:**58–63, 2000
11. Kunimatsu A, Aoki S, Masutani Y, Abe O, Mori H, Ohmoto K: Three-dimensional white matter tractography by diffusion tensor imaging in ischaemic stroke involving the corticospinal tract. **Neuroradiology 45:**532–535, 2003
12. Maier MA, Armand J, Kirkwood PA, Yang HW, Davis JN, Lemon RN: Differences in the corticospinal projection from primary motor cortex and supplementary motor area to macaque upper limb motoneurons: an anatomical and electrophysiological study. **Cereb Cortex 12:**281–296, 2002
13. Masutani Y, Aoki S: EPI distortion correction for MR-DTI by using texture memory on graphics hardware, in Lemke HU, Vannier MW, Inamura K, et al (eds): **Computer Assisted Radiology and Surgery.** Amsterdam: Excerpta Medica, 2003, p 1315
14. Masutani Y, Aoki S, Abe O, Hayashi N, Otomo K: MR diffusion tensor imaging: recent advance and new techniques for diffusion tensor visualization. **Eur J Radiol 46:**53–66, 2003
15. Mori S, Frederiksen K, van Zijl PC, Stieltjes B, Kraut MA, Solaiyappan M, et al: Brain white matter anatomy of tumor patients evaluated with diffusion tensor imaging. **Ann Neurol 51:** 377–380, 2002
16. Mori S, van Zijl PC: Fiber tracking: principles and strategies—a technical review. **NMR Biomed 15:**468–480, 2002
17. Orioli PJ, Strick PL: Cerebellar connections with the motor cortex and the arcuate premotor area: an analysis employing retrograde transneuronal transport of WGA-HRP. **J Comp Neurol 288:** 612–626, 1989
18. Wieshmann UC, Symms MR, Parker GJ, Clark CA, Lemieux L, Barker GJ, et al: Diffusion tensor imaging demonstrates deviation of fibres in normal appearing white matter adjacent to a brain tumour. **J Neurol Neurosurg Psychiatry 68:**501–503, 2000

Manuscript received June 2, 2004.

Accepted in final form November 15, 2004.

This work was supported in part by the Research Grants for Cardiovascular Disease from the Ministry of Health and Welfare of Japan and the Japan Epilepsy Research Foundation.

Address reprint requests to: Kyousuke Kamada, M.D., Department of Neurosurgery, The University of Tokyo, 7-3-1 Hongo, Bunkyo-ku, Tokyo 113-8655, Japan. email: kamady-k@umin.ac.jp.